Influence of sputtering pressure on the properties of NiO films prepared by dc reactive magnetron sputtering

A. MALLIKARJUNA REDDY[a,b,*], SEUNG KI JOO[b], A. SIVASANKAR REDDY[c], P. SREEDHARA REDDY[a]
[a]*Department of Physics, Sri Venkateswara University, Tirupati 517502, India*
[b]*Research Institute of Advanced Materials, Department of Material Science and Engineering, Seoul National University, Seoul 151-744, Republic of Korea*
[c]*Division of Advanced Materials Engineering, Kongju National University, Cheonan City, Republic of Korea*

The effect of sputtering pressure on the properties of dc reactive magnetron sputtered nickel oxide thin films was discussed in the present paper. The structural, morphological, compositional, optical and electrical properties of the deposited films were influenced by sputtering pressure. From X-ray diffractometer studies, it was observed that films were preferentially grown along (220) reflection. The films exhibited wide direct optical band gap of 3.82 eV with transmittance of 60% at the sputtering pressure of 4 Pa. Hall effect measurements showed that all films exhibited p-type conductivity and the electrical resistivity decreases with increasing the sputtering pressure up to 4 Pa, thereafter increased with sputtering pressure.

(Received May 16, 2012; accepted September 20, 2012)

Keywords: Magnetron sputtering, Sputtering pressure, X-ray diffraction, Surface morphology, Optical properties, Electrical properties

1. Introduction

Nickel oxide (NiO) with a cubic structure is a metal oxide semiconductor with anti-ferromagnetic transition. It is a promising material for applications in energy efficient smart windows [1], automobile mirrors [2], electrochromic display devices [3], p-type transparent conductive films [4], spin-valve films [5], and chemical sensors [6], due to its good chemical stability, optical and magnetic properties, NiO is considered to be a model semiconductor with p-type conductivity with wide band gap ranging from 3.6-4.0 eV [4]. The bulk NiO usually presents a non stoichiometric, Ni defective structure and shows a p-type semiconductor behavior [7]. It is evident that the improvement of the material properties can be reached by the optimization of the preparation conditions. NiO films can be fabricated by various kinds of techniques including sputtering [8-10], electron beam evaporation [11], vacuum evaporation [12], chemical bath deposition [13], sol-gel [14] and oxidation process [15]. Among these methods, dc reactive sputtering has been most widely useful technique having high deposition rates, uniformity over large areas of the substrates and easy control over the composition of the deposited films. In the present study, NiO thin films were deposited using dc reactive magnetron sputtering technique and studied the effect of sputtering pressure on the structural, morphological, compositional, optical and electrical properties.

2. Experimental

NiO thin films were grown on Corning 7059 glass substrates by using dc reactive magnetron sputtering from a homemade circular planar magnetron sputtering system. The sputtering system is capable of creating an ultimate vacuum of 5×10^{-4} Pa. The sputter chamber was pumped with diffusion pump and rotary pump combination. The pressure in the sputter chamber was measured using digital Pirani and Penning gauge combination. A circular planar magnetron of 100 mm diameter was used as the magnetron cathode. The magnetron target assembly was mounted on the top of the sputter chamber such that the sputtering could be done by sputter down configuration. A continuously variable dc power supply of 1000 V and 1 A was used as a power source for sputtering. A 100 mm diameter and 3 mm thick pure Nickel (99.98%) was used as sputter target. Pure argon was used as sputter gas and oxygen as reactive gas. The flow rates of both argon and oxygen gases were controlled individually by Tylan mass flow controllers. Before deposition of each film, the target was sputtered in pure argon atmosphere for 10 min to remove oxide layer if any on the surface of the target. NiO thin films were deposited at various sputtering pressures from 2 to 6 Pa by keeping the other deposition conditions such as substrate temperature, oxygen partial pressure and sputtering power as constant. The sputtering conditions maintained during the growth of NiO films were given in Table 1.

Table: 1 Deposition parameters maintained during the deposition of NiO films by dc reactive magnetron sputtering.

Sputtering target pure Nickel (99.98%)	100 mm diameter and 3 mm thick
Target to substrate distance	70 mm
Substrates	Corning 7059 glass
Ultimate pressure (P_U)	5 x 10^{-4} Pa
Oxygen partial pressure (pO_2)	6 x 10^{-2} Pa
Sputtering pressure (P_W)	2-6 Pa
Substrate temperature (T_S)	523 K
Sputtering power	150 W
Substrate bias voltage	0 V

The deposited films were characterized and studied the crystallographic structure, morphology, composition, optical and electrical properties. The film thickness of the deposited samples was measured by X-ray reflectivity technique. A Scinco made instrument of model SMD 3000 was used for the measurement of film thickness. The crystallographic structure of the films was analyzed by X-ray diffractometer using Cu K_α radiation (λ = 0.1546 nm) of model 3033TT manufactured by Seifert. The surface morphology was studied by atomic force microscopy (AFM) manufactured by Park systems, scanning electron microscope (SEM) of model EVO MA 15 manufactured by Carl Zeiss, for which an EDS is attached of model Inca Penta FETx3 manufactured by Oxford Instruments was used for microstructure and composition analysis. The optical properties of the films were determined by Perkin Elmer Lambda 950 UV-Vis-NIR double beam spectrophotometer. The electrical resistivity and Hall mobility were studied by employing the van der Pauw method [16]. The film thickness of all the deposited samples in the present study was around 350 nm.

3. Results and discussion

3.1. Structural properties

The X-ray diffraction patterns of the NiO films deposited at different sputtering pressures were shown in Fig.1. The crystal structures of the films at various sputtering pressures were identified to be polycrystalline and retain cubic structure.

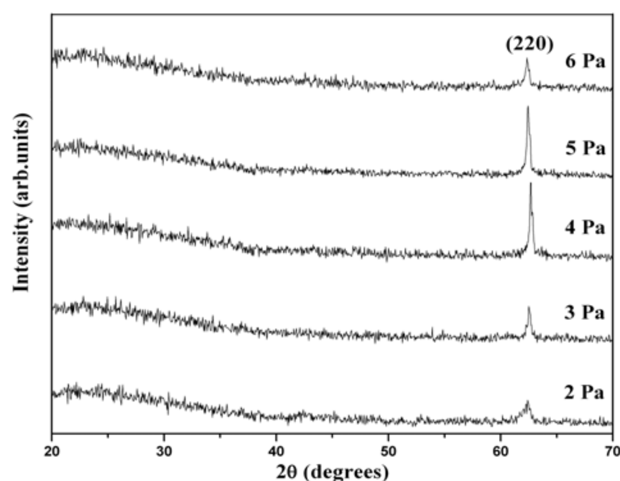

Fig.1. X-ray diffraction patterns of NiO films deposited at different sputtering pressures.

The films prepared at a sputtering pressure of 2 Pa exhibited (220) orientation. As the sputtering pressure increased to 4 Pa the intensity of (220) peak was increased and becomes sharper, on further increasing the sputtering pressure to 6 Pa, the peak width becomes wider and intensity of the (220) peak was gradually decreased. An increase in sputtering pressure decreases the plasma density, which has the effect of reducing the charging efficiency of the system but also reduces the sputtering rate. A lower charging efficiency allows more clusters to grow to a larger size via agglomeration, prior to charging [17]. The stress (σ) developed in the films was calculated from the X-ray diffraction data employing the relation [18]

$$\sigma = -E(a-a_o)/2\nu a_o \quad (1)$$

where E is the Young's modulus of the NiO (200 GPa), 'a' is the lattice parameter of the bulk material, a_o is the measured lattice parameter and ν is the Poisson's ratio (0.31). The stress developed in the films is obtained by the shift in the interplanar spacing and hence change in the lattice parameter. The tensile stress in the films decreased from 1.9959 to 1.0009 GPa with increasing the sputtering pressure from 2 to 4 Pa, thereafter it increased to 2.3773 GPa at 6 Pa, The tensile stress developed in the films was due to the existence of microscopic voids incorporated in the films during condensation [19]. The grain size of the films was calculated for (220) peak by using Scherrer's equation

$$L = \frac{K\lambda}{\beta \cos\theta} \quad (2)$$

The grain size of the films increased from 11.81 to 29.17 nm with increasing of sputtering pressure from 2 to

4 Pa thereafter it decreased to 18.98 nm at higher sputtering pressure. The increase of grain size with the increase of sputtering pressure was due to the improvement in the crystallinity of the films. The lattice parameter, grain size and stress of the NiO films as a function of sputtering pressure were given in Table 2.

Table: 2 Structural information of dc reactive magnetron sputtered NiO films at various sputtering pressures.

Sputtering pressure (Pa)	Orientation	Lattice parameter (nm)	Grain size (nm)	Stress (GPa)
2	(220)	0.4202	11.81	1.9959
3	(220)	0.4196	26.89	1.5379
4	(220)	0.4189	29.17	1.0009
5	(220)	0.4203	27.97	2.0769
6	(220)	0.4207	18.98	2.3773

3.2. Surface morphology and Composition

The AFM micrographs of NiO films deposited at various sputtering pressures were shown in Fig.2. The AFM micrograph of NiO film deposited at lower sputtering pressure of 2 Pa, the films showed non-uniform grains with surface roughness of 8.2 nm. As the sputtering pressure increased to 4 Pa, uniform grains were observed with increased surface roughness of 9.4 nm.

The decreasing of grain size and the surface roughness was observed at higher sputtering pressures. At higher sputtering pressures, the surface mobility of the adatoms decreases after series of collisions resulting in the decrease of grain size.

The scanning electron microscopy images of NiO films at different sputtering pressures were shown in Fig.3. It was observed that, smooth surface in the films was observed at a sputtering pressure of 2 Pa and the fine grains were appeared when the films were deposited at a sputtering pressure of 4 Pa. The size of the grains decreased when the films deposited beyond this sputtering pressure

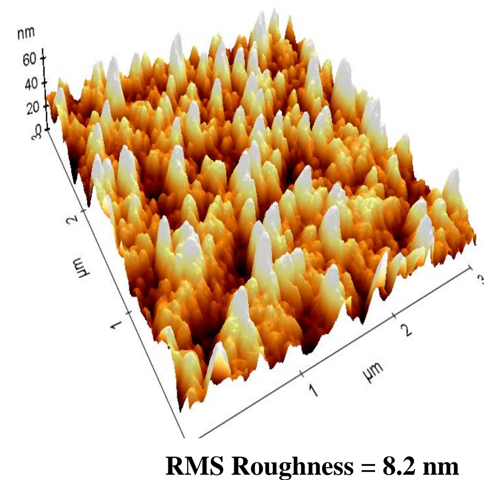

RMS Roughness = 8.2 nm

a

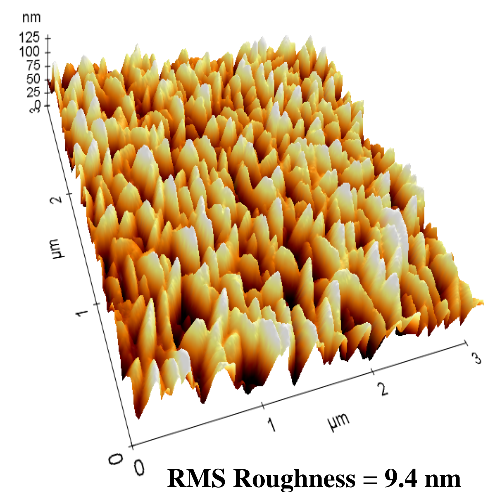

RMS Roughness = 9.4 nm

b

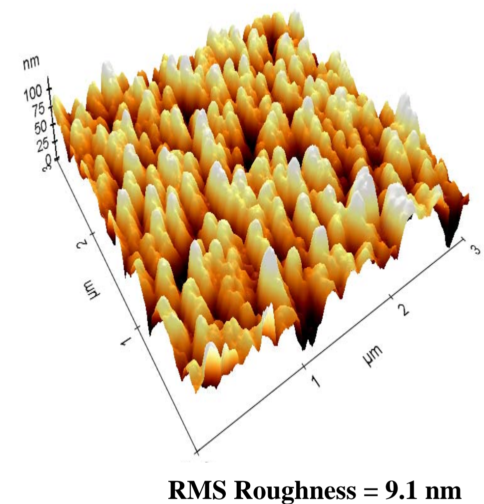

RMS Roughness = 9.1 nm

c

Fig. 2. AFM images of NiO films at sputtering pressure of (a) 2 Pa (b) 4 Pa and (b) 6 Pa

.

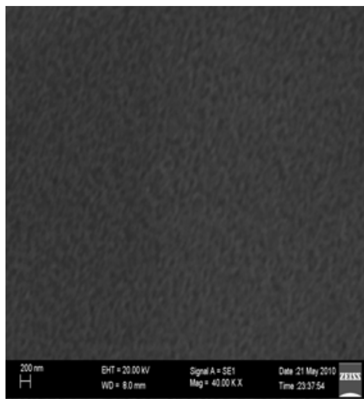

a

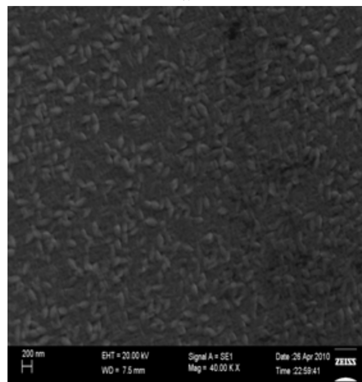

b

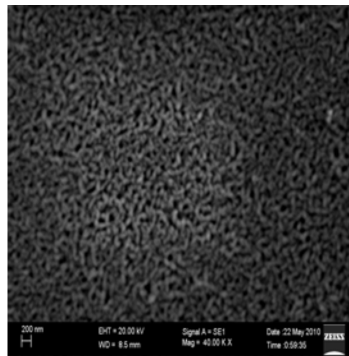

c

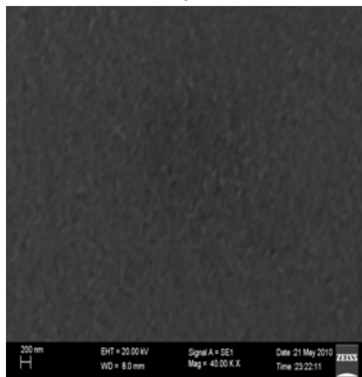

d

Fig.3. SEM images of NiO films as a function of sputtering pressure (a) 2 Pa (b) 3 Pa (c) 4 Pa and (d) 6 Pa.

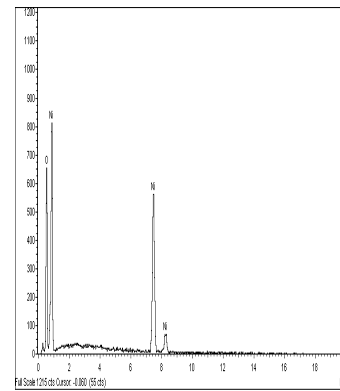

a

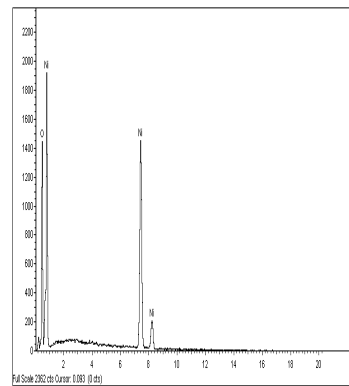

b

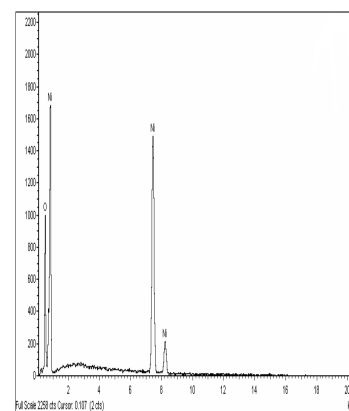

c

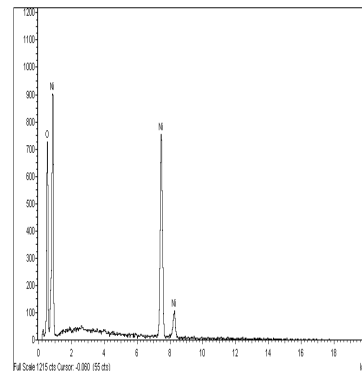

d

Fig.4. EDS spectra of NiO films deposited at various sputtering pressures (a)2 Pa (b) 3 Pa (c) 4 Pa and (d) 6 Pa.

Table: 3 The compositional analysis of dc reactive magnetron sputtered NiO films at various sputtering pressures by energy dispersive spectroscopy (EDS).

Sputtering pressure (Pa)	Element	Weight %	Atomic %	Ni/O ratio
2	O K	31.22	62.49	0.60
	Ni K	68.78	37.51	
3	O K	27.72	58.46	0.71
	Ni K	72.28	41.54	
4	O K	20.78	49.04	1.04
	Ni K	79.22	50.96	
5	O K	23.49	52.98	0.89
	Ni K	76.51	47.02	
6	O K	27.56	58.26	0.70
	Ni K	72.44	40.90	

The energy dispersive spectroscopy (EDS) was employed to identify the composition of the as deposited NiO films at different sputtering pressures. EDS results (Fig.4 & Table 3) revealed that all the deposited films consists of nickel and oxygen.

3.3. Optical properties

The optical transmittance of the films increased from 40 to 60% with increasing the sputtering pressure from 2 to 4 Pa. On further increasing the sputtering pressure to 6 Pa, the transmittance of the films decreased to 47%. The absorption edge was shifted towards lower wavelength with the increase of sputtering pressure up to 4 Pa. At lower sputtering pressures, the defect centers present in the films scatters the light and the transmittance has lower value. By increasing the sputtering pressure, the density of defect centers decreases, resulting in the increase of the transmittance value. Higher sputtering pressure leads the changing in microstructure of the films, such as the surface roughness and columnar boundaries. All these lead to the increase in light scattering. Therefore, the transmittance of films decreases at higher sputtering pressures [20]. The optical absorption coefficient (α) was calculated from the optical transmittance (T) and reflectance (R) data using the relation

$$\alpha = -1/t \quad [\ \ln T/(1-R)^2\ ] \qquad (3)$$

where t is the thickness of the film.

The dependence of α on the photon energy ($h\nu$) fitted to the relation for direct transition

$$\alpha h\nu = A\,(h\nu - E_g)^{1/2} \qquad (4)$$

where E_g is the optical band gap of the films.
The plots of $(\alpha h\nu)^2$ versus photon energy ($h\nu$) of the NiO films formed at various sputtering pressures were shown in Fig.5. The optical band gap of the films was evaluated from the extrapolation of the linear portion of the plots of $(\alpha h\nu)^2$ verses ($h\nu$) to $\alpha = 0$. The optical band gap of the films increased from 3.60 to 3.82 eV with the increase of sputtering pressure from 2 to 4 Pa. Beyond this sputtering pressure, the optical band gap of NiO films was decreased to 3.78 eV (Table 4). The optical band gap obtained at a sputtering pressure of 4 Pa in the present investigation was in good agreement with the reported rf magnetron sputtered NiO films [21]. However in the literature large optical band gap of 4.3 eV was reported by Romero et al. [22] in chemical spray pyrolysis deposited NiO films. Varkey and Fort [23] reported the lower optical band gap of 3.25 eV for NiO films coated using solution growth method.

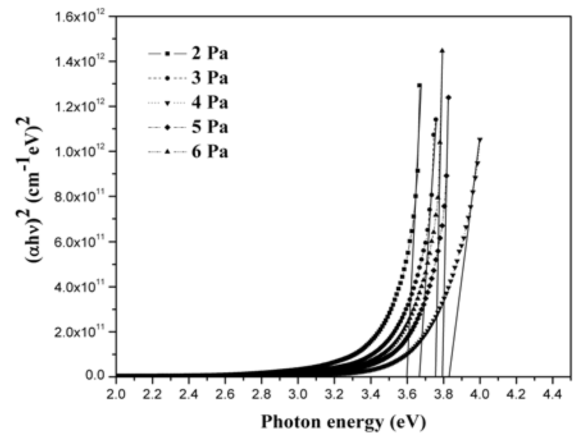

Fig.5. Plot of $(\alpha h\nu)^2$ and ($h\nu$) for the NiO films deposited at different sputtering pressures.

Table 4. Optical information of dc reactive magnetron sputtered NiO films at various sputtering pressures.

Sputtering pressure (Pa)	Transmittance (%)	Optical band gap(eV)
2	40	3.60
3	53	3.68
4	60	3.82
5	57	3.80
6	47	3.78

3.4. Electrical properties

The electrical properties of the films were highly influenced by sputtering pressure. Fig.6 shows the electrical resistivity of NiO films formed at various sputtering pressures. The electrical properties of NiO films are associated with their microstructure, composition, and the deposition environment. The electrical resistivity of the films gradually decreased from 96.2 to 5.1 Ωcm with increasing of sputtering pressure from 2 to 4 Pa. This may be due to the increase of crystallinity in NiO films. On further increasing of the sputtering pressure to 6 Pa, the

electrical resistivity of the films increased to 42.3 Ωcm. The Hall mobility measurements indicated that the films were p-type conduction. The Hall mobility and carrier concentration of the films increased from 1.5 to 4.6 $cm^2V^{-1}s^{-1}$ and 4.3 x 10^{16} to 2.6 x 10^{17} cm^{-3} with increasing the sputtering pressure from 2 to 4 Pa, respectively, and the electrical results were given in Table 5.

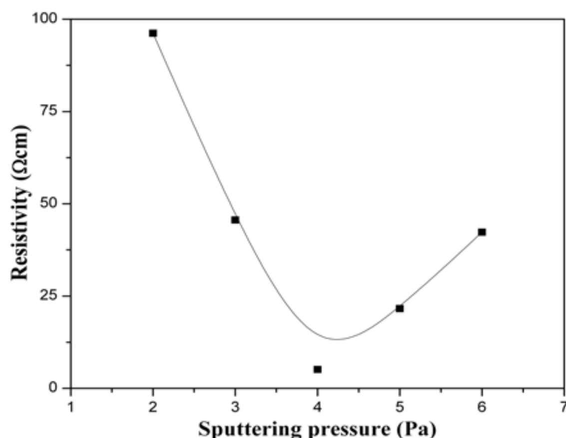

Fig.6. Variation of electrical resistivity of NiO film as a function of sputtering pressure.

The increase of Hall mobility and carrier concentration with increase of sputtering pressure was due to the improvement in grain size and the alignment of grains at the grain boundaries which minimizes the trapping and scattering of the charge carriers at the grain boundaries [24].

Table 5. Hall effect data of dc reactive magnetron sputtered NiO films at different sputtering pressures.

Sputtering pressure (Pa)	Resistivity (ρ) (Ωcm)	Carrier concen tration (n) (cm^{-3})	Mobility (μ) ($cm^2V^{-1}s^{-}$)
2	96.2	4.3 x 10^{16}	1.5
3	45.6	4.9 x 10^{16}	2.8
4	5.1	2.6 x 10^{17}	4.6
5	21.6	7.4 x 10^{16}	3.9
6	42.3	5.0 x 10^{16}	2.9

4. Conclusions

The deposited NiO films exhibited (220) preferred orientation at all sputtering pressures. The optical transmittance and band gap of the films increased from 40 to 60 % and 3.60 to 3.82 eV with increasing of sputtering pressure from 2 to 4 Pa respectively. The low electrical resistivity of 5.1 Ωcm was obtained at sputtering pressure of 4 Pa.

References

[1] C. M. Lampert, Sol. Energy Mater. Sol. Cells **76,** 489 (2003).
[2] J. Nagai, Solid State Ionics **40-41**, 383 (1990).
[3] X. P. Zhang, H.K. Zhang, Q. Li, H.L. Luo, IEEE Electron Device Lett. **21**, 215 (2000).
[4] H. Sato, T. Minami, S. Takata, T. Yamada, Thin Solid Films **236**, 27 (1993).
[5] T.C. Anthony, J. A. Brug, S. Zhang, IEEE Trans. Magn. **30**, 3819 (1994).
[6] I. Hotovy, J. Huran, L. Spiess, S. Hascik, V. Rehacek, Sens. Actuators B: Chem. **57,** 147 (1999).
[7] S. Nagakura, Iwanami Dictionary of Physics and Chemistry, 3rd Ed., Tokyo, Iwanami, 1998.
[8] G.H. Yu, L.R. Zeng, F.W. Zhu, C. L. Chai, W. Y. Lai, J. Appl. Phys. **90**, 4039 (2001).
[9] I. Hotovy, D. Buc, S. Hascik, O. Nennewitz, Vacuum **50,** 41 (1998).
[10] S. Nishizawa, T. Surumi, H. Hyodo, Y. Ishibashi, N. Ohashi, M. Yamane, O. Fukunaga, Thin Solid Films **302,** 133 (1997).
[11] A. Agarwal, H. R. Habibi, R. K. Agarwal, J. P. Cronin, D. M. Roberts, C.P.R. Sue, C. M. Lampert, Thin Solid Films **221,** 239 (1992).
[12] B. Sasi, K.G. Gopchandran, Sol. Energy Mater. Sol. Cells **91,** 1505 (2007)
[13] X. H. Xia, J.P. Tu, J. Zhang, X.L. Wang, W.K. Zhang, H. Huang, Sol. Energy Mater. Sol. Cells **92**, 628 (2008).
[14] M. Kitao, K. Izawa, K. Urabe, T. Komatsu, S. Kuwano, S. Yamada, Jpn. J. Appl. Phys. **33**, 6656 (1994).
[15] J.C. Jesus, P. Periera, J. Carrazza, F. Zaera, Surf. Sci. **369,** 217-230 (1996).
[16] L.J. van der Pauw, Philips Res. Rep. **13,** 1 (1958).
[17] M.C. Barnes, S. Kumar, L. Green, N.M. Hwang, A.R. Gerson, Surf. Coat. Technol. **190**, 321 (2005).
[18] M. Ohring, The material science of Thin Films, New York, Academic Press,1992.
[19] W. Buckel, Internal stresses, J. Vac. Sci. Technol. **6**, 606 (1969).
[20] P. Gao, L.J. Meng, M.P. dos Santos, V. Teixeira, M. Andritschky, Appl. Surf. Sci. **173**, 84 (2001).
[21] S. Nandy, U.N. Maiti, C.K. Ghosh, K.K. Chattopadhyay, J. Phys.: Condens. Matter **21**, 115804 (2009).
[22] R. Romero, F. Martin, J.R. Ramos-Barrado, D. Leinen, Thin Solid Films **518**, 4499 (2010).
[23] A. J. Varkey, A. F. Fort, Thin Solid Films **235**, 47 (1993).
[24] P. Mohan Babu, G. Venkata Rao, P. Sreedhara Reddy, S. Uthanna, J. Mater. Sci. Mater. Electronics **15**, 389 (2004).

*Corresponding author: amreddy81@gmail.com